Sterilization Effects on Ultrathin Film Polymer Coatings for Silicon-based Implantable Medical Devices

Zohora Iqbal[a,*], **Willieford Moses**[b,*], **Steven Kim**[c], **Eun Jung Kim**[a], **William H. Fissell**[d], and **Shuvo Roy**[a]

[a]Department of Bioengineering & Therapeutic Sciences, University of California - San Francisco (UCSF), San Francisco, CA, United States

[b]Department of Surgery, UCSF, San Francisco, CA, United States

[c]Division of Nephrology, UCSF, San Francisco, CA, United States

[d]Division of Nephrology and Hypertension, Vanderbilt University Medical Center, Nashville, TN, United States

Abstract

Novel biomaterials for medical device applications must be stable throughout all stages of preparation for surgery, including sterilization. There is a paucity of information on the effects of sterilization on sub-10 nm-thick polymeric surface coatings suitable for silicon-based bioartificial organs. This study explores the effect of five standard sterilization methods on three surface coatings applied to silicon: polyethylene glycol (PEG), poly(sulfobetaine methacrylate) (pSBMA), and poly(2-methacryloyloxyethyl phosphorylcholine) (pMPC). Autoclave, dry heat, hydrogen peroxide (H_2O_2) plasma, ethylene oxide gas (EtO), and electron beam (E-beam) treated coatings were analyzed to determine possible polymer degradation with sterilization. Post-sterilization, there were significant alterations in contact angle, maximum change resulting from H_2O_2 (−14°), autoclave (+15°), and dry heat (+23°) treatments for PEG, pSBMA and pMPC, respectively. Less than 5% coating thickness change was found with autoclave and EtO on PEG-silicon, E-beam on pSBMA-silicon and EtO treatment on pMPC-silicon. H_2O_2 treatment resulted in at least 30% decrease in thickness for all coatings. Enzyme-linked immunosorbent assays (ELISA) showed significant protein adsorption increase for pMPC-silicon following all sterilization methods. E-beam on PEG-silicon and dry-heat treatment on pSBMA-silicon exhibited maximum protein adsorption in each coating subset. Overall, the data suggests autoclave and EtO treatments are well-suited for PEG-silicon, while E-beam is best suited for pSBMA-silicon. pMPC-silicon was least impacted by EtO treatment. H_2O_2 treatment had a negative effect on all three coatings. These results can be used to determine which surface modifications and sterilization processes to utilize for devices *in vivo*.

Corresponding Author: Shuvo Roy, PhD, shuvo.roy@ucsf.edu, Address: Department of Bioengineering and Therapeutic Sciences, University of California - San Francisco, Byers Hall, Room 203A, MC 2520, 1700 4th Street, San Francisco, CA 94158, USA., Phone number: 415-514-9666, Fax number: 415-514-9766.
[*]These authors contributed equally to this work

Keywords

silicon; sterilization; ultrathin zwitterionic polymer (phosphorylcholine, sulfobetaine methacrylate); polyethylene glycol; non-fouling surface coatings

1. Introduction

Silicon-based devices are increasingly attractive for implantable medical applications due to their precisely-defined micro- and nanoscale features which can be produced at low unit cost and with integration of microelectronics. Some of these devices include microelectrodes for neuroprosthetics,[1] systems for controlled drug delivery,[2,3] immunoisolation chambers for cell transplants,[4–8] and filtration membranes for renal replacement therapy.[9,10] Such applications bring silicon in direct contact with body fluids, including blood. According to the US Centers for Disease Control and Prevention (CDC), any medical device that encounters sterile biological fluids is categorized as a "critical item" and must be sterilized. For implants, the guidelines require a sterility assurance level (SAL) of 10^{-6}, which is equivalent to the probability of one in a million spores surviving the sterilization process. This level can be achieved by a number of physical and chemical processes: high temperature exposure, chemical and chemical plasma exposure, and irradiation.[11] While these treatments can eradicate microbes and spores, their harsh characteristics can cause cross-linking, bond disruption, and/or oxidation of the medical device components, possibly causing unacceptable damage to functionalized surfaces.

Our team has pioneered silicon nanopore membrane (SNM) technology for the development of bioartificial organs, including an implantable bioartificial kidney,[9,12,13] and a bioartificial pancreas,[7] as shown in Figure 1. The bioartificial kidney uses uniformly sized sub-10 nm slit shaped pores produced on silicon substrates. These form a highly permeable and selective membrane, allowing for convective clearance of solutes similar to a functioning glomerulus in a healthy kidney. In the bioartificial pancreas, the SNM provides immunoisolation of encapsulated islets and protects them from the host's immune factors, while allowing the passage of glucose, insulin, and other small molecules.

Biocompatibility of the SNM is essential to successful operation of bioartificial organs *in vivo.* To this end, the biocompatibility of silicon can be enhanced by the application of ultra-thin polymeric coatings that minimize biofouling and subsequent degradation of the underlying substrate.[14–17] For our bioartificial organs, we are investigating three different surface modifications that were selected for their hydrophilicity and controllable degree of polymerization: polyethylene glycol (PEG), polysulfobetaine methacrylate (pSBMA) and poly(2-methacryloyloxyethyl phosphorylcholine) (pMPC). PEG is a widely used non-fouling surface modification.[16,18–24] It is theorized that the PEG chains produce a brush-like layer which remains hydrated and creates steric repulsion.[14,25] pSBMA and pMPC are zwitterionic polymeric brushes that have also demonstrated excellent non-fouling properties. [15,26–29] These biomimetic polymers are able to coordinate water molecules in a manner that resists protein and cell adhesion.[30]

While silicon itself may not be affected by conventional sterilization techniques such as autoclave and gamma radiation,[31] the effect of sterilization on thin-film polymeric surface coatings applied to silicon is not well characterized. Other studies have shown effects of sterilization on hydrogels, crosslinked polymers, and surface modifications that are orders of magnitude thicker.[32–34] However, to our knowledge, effect of sterilization on sub-10 nm thick brush-like polymer structures of PEG, pSBMA and pMPC have not been reported. Therefore, the purpose of this study was to investigate the effect of common sterilization modalities on silicon coated with PEG, pSBMA, and pMPC. The coated substrates were sterilized using five techniques accepted by the CDC: autoclave, dry heat, hydrogen peroxide (H_2O_2) plasma, ethylene oxide (EtO) gas, and electron beam (E-beam) irradiation. We utilized a variety of surface characterization tools to examine the physical and chemical effects of sterilization. X-ray photoelectron spectroscopy (XPS) was conducted to determine the chemical composition at the surface. Change in wettability was determined by using water contact angle, and change in polymer thickness was measured using ellipsometry. Together, these three tests give us insight into conformation change and/or degradation of the polymer chains. Finally, changes in protein resistance with and without sterilization was measured using enzyme-linked immunosorbent assays (ELISA).

2. Materials and Methods

2.1 Sample preparation

Double side polished, 400 μm thick, p-type silicon wafers were obtained from Ultrasil Corporation (Hayward, CA, USA) and diced into 1 cm^2 chips. The chips were cleaned by "piranha," a solution of 3:1 ratio of sulfuric acid (96%) to hydrogen peroxide (30%) for 20 min. Afterwards they were exposed to hydrofluoric acid for 5 min to remove the silicon dioxide that spontaneously forms on silicon surfaces exposed to atmospheric oxygen, followed by activation of the surface and another piranha clean. The silicon chips were then dried off with nitrogen gas and used immediately for surface modification.

2.2 Surface modification

2.2.1 PEG surface modification—Silicon surfaces were modified with PEG as previously described.[7,13] Briefly, substrates were dried on a hotplate at 110 °C for 1 hour. 2-[methoxy(polyethyleneoxy)propyl]trimethoxysilane (PEG-silane) (shown in Table 1), was purchased from Gelest (Morrisville, PA, USA) and covalently bonded to silicon by immersing the substrates in a solution of 285 μl PEG-silane in 25 mL of toluene for 2 hours at 70 °C. The substrates were then rinsed three times at 10 min intervals with toluene, ethanol, and water respectively, to remove excess PEG.

2.2.2 Zwitterionic surface modification—All chemicals were purchased from Sigma-Aldrich (St. Louis, MO, USA), unless stated otherwise. Zwitterionic surface modifications were conducted as previously published.[35] Briefly, a surface initiator 2-bromo-2-methyl-N-3[(trimethoxysilyl)propyl]-propanamide (BrTMOS) as shown in Table 1, was synthesized.[35] The substrates were placed in a 1% (v/v) BrTMOS solution in bicyclohexyl for 2 hours. The surfaces were then rinsed with chloroform, ethanol, and water respectively, to remove excess BrTMOS.

2-(methacryloyloxy)ethyl]dimethyl-(3-sulfopropyl)ammonium hydroxide (SBMA), and 2-methacryloyloxyethyl phosphorylcholine (MPC), are shown in Table 1 respectively. A degassed solution of 468 mg (3 mmol) of 2,2′-bipyridyl (98%) and individual monomers—SBMA: 1.06g (3.8 mmol), and MPC: 506 mg (1.9 mmol)—and 22.3 mg (0.1 mmol) of copper (II) bromide (99%) was prepared in 5:5 mL of methanol:water. This mixture was added to a reaction chamber housing four substrates and 143 mg (1 mmol) of copper (I) bromide (99.999%) under nitrogen protection, and polymerization ran for 15 min for pSBMA and 7 min for pMPC. The substrates were then rinsed with chloroform, ethanol, Dulbecco's phosphate buffered saline (D-PBS, UCSF Cell Culture Facility, San Francisco, CA, USA), and water respectively, and dried using a stream of nitrogen gas.

2.2.3 Sterilization processes—Five sterilization processes were evaluated. Autoclave was conducted using STERIS Amsco Century, SV-120 Scientific Prevacuum Sterilizer (Mentor, OH, USA), exposing the substrates to high pressure steam for 30 minutes at 121 °C. For dry heat sterilization, substrates were placed in a 160 °C oven for 2 hours.[36] H_2O_2 plasma treatment was conducted using STERRAD® 100S Sterilization System (standard cycle). EtO gas treatment was conducted by D_2EO (San Jose, CA, USA) with a 2-hour exposure time at 132 mBar and 55°C. Lastly, E-beam sterilization was performed by STERIS (Petaluma, CA, USA), at an applied dosage range of 21.0 to 21.9 kGy.

2.2.4 Surface characterization

<u>**XPS:**</u> XPS was conducted using a Surface Science Instruments S-Probe spectrometer with a monochromatized Al Kα X-ray beam. A pass energy of 150 eV was used to generate the survey and high resolution spectra. Samples were pressurized to <5e-9 torr and a 0° take-off angle was used, corresponding to sampling depth of ~10 nm. For each sample, XPS was measured at three locations with a spot size of ~800 μm. Elemental composition calculations were performed using Service Physics Hawk version 7 software (Bend, OR, USA).

<u>**Contact angle:**</u> Change in surface hydrophilicity was measured using sessile drop contact angle goniometry (Attension Theta Lite, Biolin Scientific, Stockholm, Sweden). A ~3.5 μl water droplet was placed on the substrate in air and the contact angle between the droplet and the substrate was measured. Data points was collected every 0.1 s over 10 s, and averaged. A total of six data points was collected from each sample subset.

<u>**Ellipsometry:**</u> Surface coating thickness was measured using a LSE Stokes ellipsometer (Gaertner Scientific, Skokie, IL, USA) with a 6328 Å HeNe laser at an incidence angle of 70°. Measured reflection and transmission data was entered into Fresnel equations and with known refractive index, thickness of the transparent film was iteratively solved for. In case of both zwitterionic and PEG surface coatings, an index of refraction of 1.45 was used.[35] Although sterilization processes may lead to conformational changes and cross-linking within the polymers, refractive index was assumed to be constant. Spatial homogeneity was characterized by measuring three locations on three separate chips per sample set. A total of 9 measurements were averaged, and the mean and standard deviation is reported.

ELISA: Resistance to protein adsorption was assessed by incubating the substrates in a 1 mg/mL solution of human serum albumin (HSA) in D-PBS for 90 minutes at 37°C. Surface protein concentrations were measured using ELISA using published methods.[27,35] Briefly, all substrates were rinsed 5 times with 0.5 mL of D-PBS following HSA incubation, and were blocked using bovine serum albumin[37] (BSA, 98%, Sigma-Aldrich) at 1 mg/mL concentration for 1.5 hours. The substrates were rinsed 5 times with 0.5 mL of D-PBS, and transferred to fresh chambers. The samples were then incubated with 10 μg/mL anti-human serum albumin antibody conjugated with horseradish peroxidase for 1.5 hours (Abcam, Cambridge, MA, USA). After another rinse (5 times with 0.5 mL of D-PBS), the substrates again rinsed and transferred to fresh chambers. A solution of 0.5 mg/mL of o-phenylenediamine (OPD, VWR Inc. Visalia, CA, USA) and 0.03% hydrogen peroxide in 0.05 M citrate phosphate buffer (pH 5.0, Sigma-Aldrich). This reaction was protected from light using aluminum foil for 20 min at 37 °C, and subsequently stopped by adding 0.5 mL of 1M sulfuric acid. The light absorbance of the solutions was measured at 490 nm. Each sample type was tested in triplicate and the background (control with no HSA added) was subtracted. All HSA protein adsorption data was normalized to tissue culture polystyrene (TCPS) which was used as a positive control.

2.2.5 Statistical Analysis—A minimum of three measurements were collected for all samples in each analysis. Statistical significance was determined by ordinary one-way analysis of variance (ANOVA) since comparisons were drawn only within each coating subset. Significance was defined at $p < 0.05$. Analysis was conducted using Graphpad Prism software (San Diego, CA, USA).

3. Results

3.1 X-ray photoelectron spectroscopy (XPS)

A comparison of survey XPS spectra for each of the unsterilized substrate types is shown in Supplementary Figure 1. Supplementary Figure 2(a) – (d) present the corresponding spectra after the various sterilization methods for each of the surface modifications, and the elemental composition is summarized in Table 2. An example of high resolution XPS data is presented in Supplementary Table 1. As expected, there is a presence of Si 2p (100 eV) and O 1s (528 eV) peaks from the monocrystalline silicon substrate and native silicon dioxide, respectively for all cases. The unmodified (uncoated) silicon also shows a presence of ~8% adventitious carbon, with the exception of H_2O_2 plasma treated substrates, where the carbon content was ~16%. After H_2O_2 plasma treatment, the unmodified silicon exhibits an elevated level of oxygen as well as a presence of nitrogen, sodium and fluorine. Since these contaminant elements are not significantly present on the other substrates, it is possible that their presence resulted from sample mishandling. Apart from H_2O_2 treated samples, high resolution data shows less than 5% change in crystalline silicon and silicon dioxide content between sterilized and unsterilized silicon substrates.

With PEG-coupled silicon, the concentration of Si 2p decreased by ~12% and O 1s and C 1s increased by ~3% and ~11%, respectively. High resolution data (Supplementary Table 1) shows the increase in carbon is due mainly due to an increase in C-O bonds, which is

expected in PEG coatings.[25] After sterilization, a slight decrease in carbon content was observed, ranging between ~11% and ~16% compared to ~18% seen in the unsterilized counterpart. Except for dry heat treated samples, this decrease in carbon is mainly reflected in reduced C-O bonds. Overall, the maximum C-O bonds was present after dry heat treatment, while H_2O_2 plasma sterilization exhibited the minimum C-O bonds. Nonetheless, percent of C-O bonds are still greater in all sterilized samples compared to unmodified silicon, indicating presence of some PEG on all sterilized substrates.

Compared to unmodified silicon, pSBMA-coupled silicon exhibited a sharp decrease in Si 2p concentration by >40%, and an increase in C 1s content by >37%. There is also a presence of signature elements, N 1s (~400 eV) and S 2s (~228 eV), as well as Br 3d (~69 eV), indicating pSBMA surface modification was successful. Additionally, high resolution XPS data (Supplementary Table 1) shows a 3.1% NR_3^+ concentration and a 2.9% sulfur concentration, which is a ratio of ~1:1 as expected from stoichiometric pSBMA. After sterilization, silicon concentration of these samples slightly decreased, ranging from ~11% to ~17% compared to the 20% silicon content of the unsterilized pSBMA substrates. However, concentration of carbon, oxygen, nitrogen and sulfur remained comparable or higher than the unsterilized counterparts. There is also a negligible amount of phosphorus contaminant present (<1%) for E-beam sterilized and non-sterilized substrates.

Unsterilized pMPC-coupled silicon shows a decrease in Si 2p and an increase in C 1s content, as expected. There is also a presence of P 2s (~190 eV) and N 1s, which are the signature elements for pMPC, suggesting successful polymerization on the silicon surface. High resolution XPS data (Supplementary Table 1) shows a 1.7% NR_3^+ concentration and a 1.2% phosphorus concentration, yielding a ratio of ~1:1, which is consistent with pMPC stoichiometric ratio. Overall, sterilization of pMPC-silicon did not result in a large change in elemental composition, except in case of H_2O_2 treatment. With H_2O_2 plasma sterilization, a maximum drop in carbon concentration was observed, as well as the minimum level of phosphorus and nitrogen. It should also be noted that the concentration of carbon is lower and silicon is higher in pMPC substrates compared to pSBMA substrates, indicating a lower degree of polymerization for pMPC than for pSBMA.

3.2 Contact angle

Contact angle data are presented in Figure 2. The sessile water droplet was stable over 10 seconds. The uncoated silicon substrate has a contact angle of 32°. With a PEG surface modification, the contact angle increased to 43°. Zwitterionic coatings showed a decrease in contact angle to 15° and 25° for pSBMA and pMPC, respectively. As is reflected by the contact angle measurements, all three surface modifications are hydrophilic. However, significant changes in hydrophilicity are observed with sterilization treatments, especially for uncoated and pMPC-coated substrates. The contact angle for pSBMA-silicon was most affected by autoclave, increasing by 15°. PEG-silicon was most affected by peroxide treatment, decreasing by 14°.

3.3 Ellipsometry

Using ellipsometry, thicknesses for the various surface coatings were determined as shown in Figure 3. The starting thickness for each of the coatings are 0.9, 7.1 and 2.7 nm for PEG, pSBMA and pMPC coatings, respectively. Statistically significant differences were observed for all coatings when sterilized with H_2O_2 plasma. Table 3 presents the thickness change relative to the unsterilized control samples, revealing substantial reduction in coating thickness following several sterilization processes. PEG-silicon decreased by >30% by dry heat, peroxide and E-beam irradiation treatment, while pSBMA and pMPC exhibited >20% thickness change with dry heat and peroxide treatment. Moreover, pSBMA was also greatly affected by steam treatment in the autoclave, decreasing in thickness by 29%.

3.4 ELISA

HSA protein adsorption data, shown in Figure 4, illustrate that both unsterilized pSBMA and pMPC coated silicon chips display excellent non-fouling properties, reducing protein adsorption by 90% and 95%, respectively compared with uncoated silicon. In contrast, PEG-coated chips only yielded a reduction by 10% compared to uncoated silicon.

Overall, none of the sterilization processes caused a significant change in protein adsorption for uncoated silicon. For the surface-modified silicon, sterilization appeared to adversely affect the coatings as evidenced by increased protein fouling. E-beam radiation on PEG-silicon caused a significant increase in HSA adsorption compared to its unsterilized counterpart. For pSBMA-silicon, dry heat and EtO treatment significantly increased HSA adsorption. Lastly, all methods of sterilization tested caused a significant increase in albumin adsorption for the pMPC-silicon surfaces.

4. Discussion

For the successful development of implantable medical devices, the effect of sterilization on the device and its surface modifications must be considered. For this study, we evaluated the effects of five common sterilization modalities for three ultrathin surface modifications on silicon—PEG, pSBMA and pMPC.[7,9,35] These polymer films are less than 10 nm thick, and are grafted to/from the surface in brush-like structures, with the presence of charged moieties in the case of zwitterionic polymers (pSBMA and pMPC). Since sterilization processes are harsh treatments that eliminate living organisms, it is anticipated that they could adversely affect the chemical and physical characteristics of the polymers and their function.

Autoclave and dry heat are the two high-temperature sterilization processes tested in this study. For polymers, high temperature can lead to thermal degradation via oxidation, as well as molecular rearrangement and cross-linking, affecting chemical properties.[38,39] Although autoclave is the most widely used sterilization method for medical instruments, steam affects the surface energy of many polymers through spontaneous rearrangement, leading to a change in their hydrophilicity.[40]

In contrast, H_2O_2, EtO and E-beam are all room temperature treatments. Nonetheless, H_2O_2 plasma sterilization is a fairly corrosive process: reactive free radicals bombard the surfaces

to kill microbes. Additionally, it has also been shown to modify exposed surfaces, reducing polymer strength, morphology, composition and wettability.[40] Toxic EtO gas sterilization is generally used in the medical field for devices that cannot withstand steam, dry heat or irradiation. However, it can leave behind dissolved residues in polymers, which requires long aeration periods post-sterilization.[41] Lastly, E-beam sterilization utilizes a beam of charged electrons that alters the chemical bonds in biological materials such as DNA strands, leading to chain scission and crosslinking.[42]

Considering these sterilization processes denature, crosslink, and degrade chemical structures in living things, it is evident that polymers, especially ultrathin surface coatings, may experience significant changes in their properties. Therefore, to analyze alterations in these polymers due to sterilization, the change in their hydrophilicity, elemental composition, thickness and non-fouling capacity was measured. Table 4 summarizes the effect of sterilization on each surface modification based on hydrophilicity, coating thickness, and protein resistance.

PEG-silicon

Compared to unsterilized silicon, unsterilized PEG-silicon only exhibited a 11% reduction in protein adsorption. Previous literature has demonstrated that PEG on silicon can reduce albumin adsorption by 75% compared to its silicon counterparts.[19,43] We confirmed presence of PEG on silicon surface through chemical composition, contact angle and thickness analyses. However, PEG chain length and surface grafting density can affect protein resistance, and the "graft to" method used in this study for PEG surface modification generally yields poor surface density compared to "graft from" method.[44] Therefore, our low reduction in protein adsorption could be due to low grafting density.

PEG coating on silicon was least affected by autoclave and EtO treatments, while dry heat, H_2O_2, and E-beam treatments affected its properties and protein resistance. When compared within the PEG subset, dry heat, H_2O_2, and E-beam treatments cause 32, 64, and 47% decrease in coating thickness, respectively. Additionally, with the exception of dry heat treatment, all other sterilization processes show a decrease in C-O bonds via XPS analysis. The negative physical and chemical surface changes correlate with ELISA data, which exhibit a corresponding increase in protein adsorption. H_2O_2 plasma also resulted in a significant decrease in hydrophilicity, which may be indicative of chain scission and ionization of PEG polymers after treatment. Despite lowered C-O bonds, when all metrics are considered, EtO and autoclave appeared to have minimal effects on PEG coatings.

pSBMA-silicon

The surface elemental composition and coating thickness of pSBMA-silicon indicates a possible change in pSBMA polymer chain conformation or crosslinking after sterilization. XPS data exhibited a decrease in silicon and an increase in carbon content after all five sterilization processes. There is also an increase in nitrogen and sulfur, which are the signature elements of pSBMA. Except for E-beam sterilization, there was a decrease in coating thickness for the sterilized substrates. While some part of the decrease in coating thickness could be due to chain scission of the polymers, the lower thickness coupled with

the increase in pSBMA signature elements in XPS demonstrates a compression of the polymer layer from crosslinking or conformational change. To examine crosslinking thoroughly, swelling behavior of the polymers may be the subject of a future study. Nonetheless, we did not see a significant negative impact in protein resistance due to these possible alterations.

Of the three surface modifications examined, pSBMA had the highest initial coating thickness, measuring 7.1 nm for the unsterilized control samples. It is possible that the polymer chain length allowed conformational and crosslinking changes to occur without compromising its effectiveness at protein resistance.

E-beam sterilization had the lowest impact on pSBMA coating, while autoclave, dry heat, H_2O_2 or EtO treatments exhibited mixed low, moderate and severe impacts on various properties. When the sterilization groups are compared within the subset of pSBMA samples, XPS showed the lowest carbon concentration for H_2O_2 plasma treated samples, followed by EtO. H_2O_2 treated samples also exhibited the lowest contact angle and the greatest change in thickness, a decrease of over 43%. This change indicates possible chain scission. However, it appears that the non-fouling property of pSBMA was still preserved since the original polymer coating thickness was greater than the damage caused by these sterilization processes.

pMPC-silicon

All five sterilization methods tested adversely affected pMPC-coatings. Except for EtO treatment, all sterilization methods resulted in at least 10% change in pMPC coating thickness, with a maximum change of 30% decrease using H_2O_2 treatment. However, XPS results show minor change in carbon concentration when compared to unsterilized samples. Unlike the pSBMA, the pMPC chains are shorter (2.7 nm thick for unsterilized substrates) and their resulting lower degree of freedom would limit alterations in chain conformation. There was a significant drop in carbon concentration for the H_2O_2 treated pMPC samples (31% to 25%), indicating possible chain scission and polymer degradation. Overall, all methods of sterilization tested led to substantial increase in contact angle and protein adsorption for pMPC-silicon substrates. However, with a thicker coating, it is possible the damage done by sterilization may have been more tolerable. Based on the results, EtO treatment had the least adverse effects on pMPC samples.

5. Conclusions

Sterilization can be especially harsh on polymer surface modifications on implantable medical devices. Therefore, we have presented data examining the effects of various sterilization processes on thin-film polymeric brushes on silicon. Our study shows H_2O_2 plasma treatment adversely affected all three polymer coatings. In contrast, autoclave and EtO treatment appear suitable for PEG, E-beam sterilization for pSBMA, and EtO treatment for pMPC coatings. These results will be useful for any silicon medical devices that utilizes ultrathin zwitterionic or PEG coatings for their applications.

As novel polymers and functional surfaces become more prevalent in medical devices, how sterilization might affect them must be assessed. Our results illustrate that these effects are unique to the surface coating chemical and physical properties. Therefore, this work presents a guideline for determining the effects of sterilization on any surface modification.

Supplementary Material

Refer to Web version on PubMed Central for supplementary material.

Acknowledgments

References

1. Cheung KC, Renaud P. BioMEMS for medicine: On-chip cell characterization and implantable microelectrodes. Solid State Electron. 2006; 50(4):551–557. DOI: 10.1016/j.sse.2006.03.023

2. Shawgo RS, Grayson ACR, Li Y, Cima MJ. BioMEMS for drug delivery. Curr Opin Solid State Mater Sci. 2002; 6(4):329–334. DOI: 10.1016/S1359-0286(02)00032-3

3. Desai T, Sharma S, Walczak R, et al. Nanoporous Implants for Controlled Drug Delivery. Ther Micro/Nano Technol - BioMEMS Biomed Nanotechnol. 2007; :263–286. DOI: 10.1007/978-0-387-25844-7_15

4. Desai TaHansford DJ, Ferrari M. Micromachined interfaces: New approaches in cell immunoisolation and biomolecular separation. Biomol Eng. 2000; 17:23–36. DOI: 10.1016/S1389-0344(00)00063-0 [PubMed: 11042474]

5. Smith C, Kirk R, West T, et al. Diffusion characteristics of microfabricated silicon nanopore membranes as immunoisolation membranes for use in cellular therapeutics. Diabetes Technol Ther. 2005; 7(1):151–162. DOI: 10.1089/dia.2005.7.151 [PubMed: 15738713]

6. Desai TaHansford D, Ferrari M. Characterization of micromachined silicon membranes for immunoisolation and bioseparation applications. J Memb Sci. 1999; 159:221–231. DOI: 10.1016/S0376-7388(99)00062-9

7. Song S, Faleo G, Yeung R, et al. Silicon nanopore membrane (SNM) for islet encapsulation and immunoisolation under convective transport. Sci Rep. 2016; 6(January):23679.doi: 10.1038/srep23679 [PubMed: 27009429]

8. Song S, Blaha C, Moses W, et al. An intravascular bioartificial pancreas device (iBAP) with silicon nanopore membranes (SNM) for islet encapsulation under convective mass transport. Lab Chip. 2017; doi: 10.1039/C7LC00096K

9. Roy S, Dubnisheva A, Eldridge A. , et al. Silicon nanopore membrane technology for an implantable artificial kidney. TRANSDUCERS 2009 - 15th Int Conf Solid-State Sensors, Actuators Microsystems; 2009; 755–760.

10. Striemer CC, Gaborski TR, McGrath JL, Fauchet PM. Charge- and size-based separation of macromolecules using ultrathin silicon membranes. Nature. 2007; 445(February):749–753. DOI: 10.1038/nature05532 [PubMed: 17301789]

11. Rutala WA, Weber DJ. Guideline for Disinfection and Sterilization in Healthcare Facilities, 2008. Clin Infect Dis. 2008; :1–158. DOI: 10.1086/423182

12. Fissell WH, Roy S. The implantable artificial kidney. Semin Dial. 2009; 22(6):665–670. DOI: 10.1111/j.1525-139X.2009.00662.x [PubMed: 20017839]

13. Kim S, Feinberg B, Kant R, et al. Diffusive silicon nanopore membranes for hemodialysis applications. PLoS One. 2016; 11(7):1–20. DOI: 10.1371/journal.pone.0159526

14. Muthusubramaniam L, Lowe R, Fissell WH, et al. Hemocompatibility of silicon-based substrates for biomedical implant applications. Ann Biomed Eng. 2011; 39(4):1296–1305. DOI: 10.1007/s10439-011-0256-y [PubMed: 21287275]

15. Nakabayashi N, Williams DF. Preparation of non-thrombogenic materials using 2-methacryloyloxyethyl phosphorylcholine. Biomaterials. 2003; 24:2431–2435. DOI: 10.1016/S0142-9612(03)00113-3 [PubMed: 12699681]

16. Fissell WH, Dubnisheva A, Eldridge AN, Fleischman AJ, Zydney AL, Roy S. High-performance silicon nanopore hemofiltration membranes. J Memb Sci. 2009; 326:58–63. DOI: 10.1016/j.memsci.2008.09.039 [PubMed: 20054402]

17. Melvin ME, Fissell WH, Roy S, Brown DL. Silicon induces minimal thromboinflammatory response during 28-day intravascular implant testing. ASAIO J. 2010; 56(4):344–348. DOI: 10.1097/MAT.0b013e3181d98cf8 [PubMed: 20431483]

18. Popat KC, Desai Ta. Poly(ethylene glycol) interfaces: An approach for enhanced performance of microfluidic systems. Biosens Bioelectron. 2004; 19:1037–1044. DOI: 10.1016/j.bios.2003.10.007 [PubMed: 15018959]

19. Zhang M, Desai T, Ferrari M. Proteins and cells on PEG immobilized silicon surfaces. Biomaterials. 1998; 19:953–960. DOI: 10.1016/S0142-9612(98)00026-X [PubMed: 9690837]

20. Li J, Tan D, Zhang X, et al. Preparation and characterization of nonfouling polymer brushes on poly(ethylene terephthalate) film surfaces. Colloids Surf B Biointerfaces. 2010; 78(2):343–350. DOI: 10.1016/j.colsurfb.2010.03.027 [PubMed: 20399623]

21. Hanein Y, Pan YV, Ratner BD, Boèhringer KF, Denton DD. Micromachining of non-fouling coatings for bio - MEMS applications. 2001; 81:2001.

22. Ma H, Hyun J, Stiller P, Chilkoti A. "Non-Fouling" Oligo(ethylene glycol)- Functionalized Polymer Brushes Synthesized by Surface-Initiated Atom Transfer Radical Polymerization. Adv Mater. 2004; 16(4):338–341. DOI: 10.1002/adma.200305830

23. Zhu X, Loo HE, Bai R. A novel membrane showing both hydrophilic and oleophobic surface properties and its non-fouling performances for potential water treatment applications. J Memb Sci. 2013; 436:47–56. DOI: 10.1016/j.memsci.2013.02.019

24. Wagner VE, Koberstein JT, Bryers JD. Protein and bacterial fouling characteristics of peptide and antibody decorated surfaces of PEG-poly(acrylic acid) co-polymers. Biomaterials. 2004; 25(12):2247–2263. DOI: 10.1016/j.biomaterials.2003.09.020 [PubMed: 14741590]

25. Sharma S, Johnson RW, Desai Ta. XPS and AFM analysis of antifouling PEG interfaces for microfabricated silicon biosensors. Biosens Bioelectron. 2004; 20(2):227–239. DOI: 10.1016/j.bios.2004.01.034 [PubMed: 15308226]

26. Zhang Z, Zhang M, Chen S, Horbett Ta, Ratner BD, Jiang S. Blood compatibility of surfaces with superlow protein adsorption. Biomaterials. 2008; 29:4285–4291. DOI: 10.1016/j.biomaterials.2008.07.039 [PubMed: 18722010]

27. Zhang Z, Chao T, Chen S, Jiang S. Superlow fouling sulfobetaine and carboxybetaine polymers on glass slides. Langmuir. 2006; 22(12):10072–10077. DOI: 10.1021/la062175d [PubMed: 17107002]

28. Chen S, Liu L, Jiang S. Strong resistance of oligo(phosphorylcholine) self-assembled monolayers to protein adsorption. Langmuir. 2006; 22(6):2418–2421. DOI: 10.1021/la052851w [PubMed: 16519431]

29. Zhang Z, Chao T, Liu L, Cheng G, Ratner BD, Jiang S. Zwitterionic hydrogels: an in vivo implantation study. J Biomater Sci Polym Ed. 2009; 20(13):1845–1859. DOI: 10.1163/156856208X386444 [PubMed: 19793443]

30. Smith RS, Zhang Z, Bouchard M, et al. Vascular catheters with a nonleaching poly-sulfobetaine surface modification reduce thrombus formation and microbial attachment. Sci Transl Med. 2012; 4(153):153ra132.doi: 10.1126/scitranslmed.3004120

31. Kotzar G, Freas M, Abel P, et al. Evaluation of MEMS materials of construction for implantable medical devices. Biomaterials. 2002; 23(13):2737–2750. http://www.ncbi.nlm.nih.gov/pubmed/12059024. [PubMed: 12059024]

32. Brétagnol F, Rauscher H, Hasiwa M, et al. The effect of sterilization processes on the bioadhesive properties and surface chemistry of a plasma-polymerized polyethylene glycol film: XPS

characterization and L929 cell proliferation tests. Acta Biomater. 2008; 4(6):1745–1751. DOI: 10.1016/j.actbio.2008.06.013 [PubMed: 18676191]

33. Kyomoto M, Moro T, Miyaji F, et al. Enhanced Wear Resistance of Orthopaedic Bearing Due to the Cross-Linking of Poly(MPC) Graft Chains Induced by Gamma-Ray Irradiation. J Biomed Mater Res B Appl Biomater. 2007; 84B:320–327. DOI: 10.1002/jbmb

34. Kanjickal D, Lopina S, Evancho-Chapman MM, Schmidt S, Donovan D. Effects of sterilization on poly(ethylene glycol) hydrogels. J Biomed Mater Res - Part A. 2008; 87(3):608–617. DOI: 10.1002/jbm.a.31811

35. Li L, Marchant RE, Dubnisheva A, Roy S, Fissell WH. Anti-biofouling Sulfobetaine Polymer Thin Films on Silicon and Silicon Nanopore Membranes. J Biomater Sci Polym Ed. 2011; 22:91–106. DOI: 10.1163/092050609X12578498982998 [PubMed: 20546677]

36. Centers for Disease Control and Prevention. [Accessed May 6, 2017] Guidelines for Disinfection and Sterilization in Healthcare Facilities (Other Sterilization Methods). https://www.cdc.gov/infectioncontrol/guidelines/disinfection/sterilization/other-methods.html. Published 2016

37. Huang Y, Lü X, Qian W, Tang Z, Zhong Y. Competitive protein adsorption on biomaterial surface studied with reflectometric interference spectroscopy. Acta Biomater. 2010; 6(6):2083–2090. DOI: 10.1016/j.actbio.2009.12.035 [PubMed: 20026435]

38. Krzysztof P, James N. Thermal Degradation of Polymeric Materials. 1. Shawbury, UK: iSmithers Rapra Publishing; 2005.

39. Han S, Kim C, Kwon D. Thermal/oxidative degradation and stabilization of polyethylene glycol. Polymer (Guildf). 1997; 38(2):317–323. DOI: 10.1016/S0032-3861(97)88175-X

40. Kubyshkina G, Zupan i B, Štukelj M, Grošelj D, Marion L, Emri I. The influence of different sterilization techniques on the time-dependent behavior of polyamides. J Biomater Nanobiotechnol. 2011; 2(4):361–368. DOI: 10.4236/jbnb.2011.24045

41. Gilding DK, Reed AM, Baskett SA. Ethylene oxide sterilization: effect of polymer structure and sterilization conditions on residue levels. Biomaterials. 1980; 1(3):145–148. DOI: 10.1016/0142-9612(80)90037-X [PubMed: 7470566]

42. Silindir M, Özer AY. Sterilization methods and the comparison of E-beam sterilization with gamma radiation sterilization. Fabad J Pharm Sci. 2009; 34(1):43–53.

43. Zhang M, Ferrari M. Hemocompatible polyethylene glycol films on silicon. Biomed Microdevices. 1998. http://www.springerlink.com/index/H6K15PK44618078T.pdf

44. Yeh P-Y, Kizhakkedathu JN, Chiao M. A Novel Method to Attenuate Protein Adsorption Using Combinations of Polyethylene Glycol (PEG) Grafts and Piezoelectric Actuation. J Nanotechnol Eng Med. 2010; 1(November 2010):41010.doi: 10.1115/1.4002532
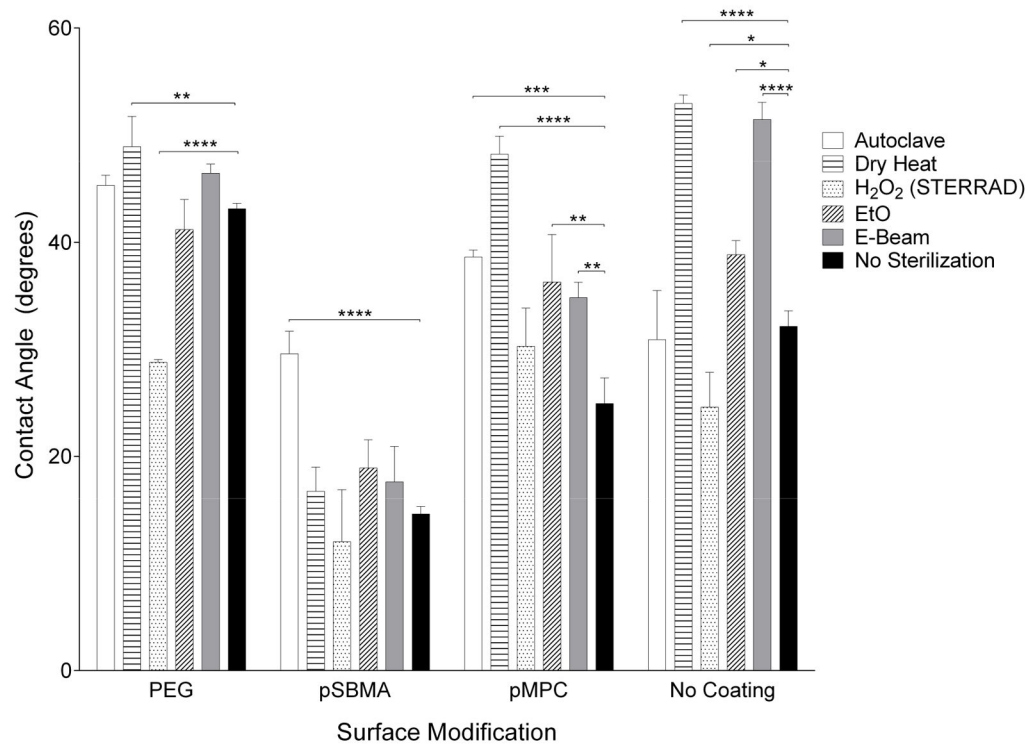
Figure 1.
Silicon nanopore membrane (SNM) developed for bioartificial organs. SNM (a) top view depicting pore length of 2 μm and pore width of 7 nm, and (b) side view depicting 360 nm pore height, reprinted from S. Song et al./Scientific Reports (6), ©2016, with permission from Nature Publishing Group (c) Concept of an artificial kidney based on SNM renal replacement therapy. (d) Immunoisolation chamber for encapsulated islets in a bioartificial pancreas.
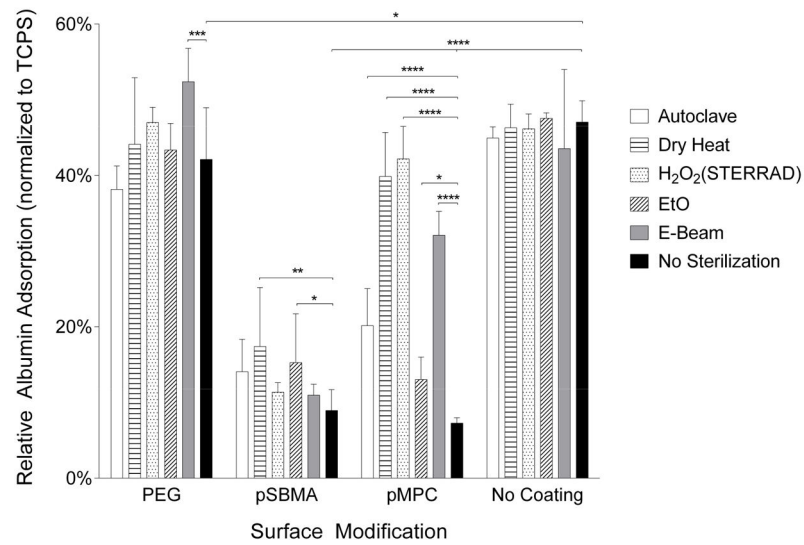
Figure 2.
Contact angle measurements before and after sterilization for surface modifications and unmodified silicon. Hydrophilicity—a fundamental property of the surface modification—of PEG was most affected by H_2O_2 plasma, pSBMA by autoclave, and pMPC by dry heat.
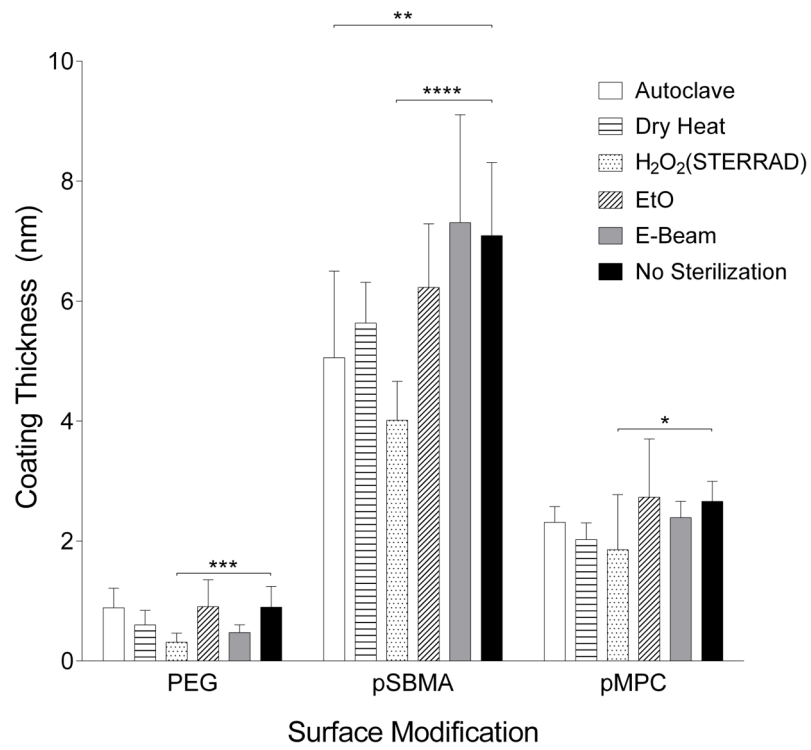
Figure 3.
Coating thickness measured by ellipsometry for PEG, pSBMA and pMPC. Change in coating thickness could be due to chain scission or polymer conformation change. Largest decrease in thickness for all three coatings was due to peroxide treatment.
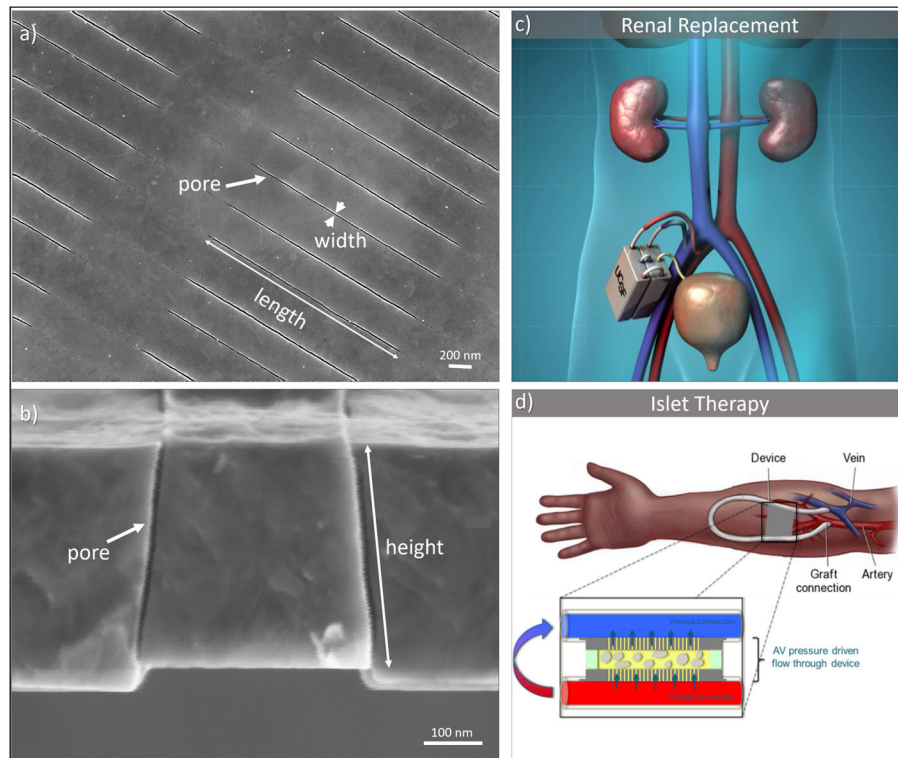
Figure 4.
Relative human serum albumin (HSA) adsorption on PEG, pSBMA and pMPC-modified and unmodified silicon surfaces. Data has been normalized to tissue culture polystyrene (TCPS). There is a statistically significant reduction in protein adsorption with surface modification. Following sterilization, protein adsorption generally increases, and significant changes with $p < 0.05$ is noted.